Research Square

Preprints are preliminary reports that have not undergone peer review.
They should not be considered conclusive, used to inform clinical practice,
or referenced by the media as validated information.

Direct hybridization facilitates the simultaneous identification and introgression of QTL for adult plant resistance to the Ug99 stem rust lineage from tetraploid Khorasan wheat to common wheat

Max Fraser (frase093@umn.edu)
University of Minnesota Twin Cities College of Food Agricultural and Natural Resource Sciences https://orcid.org/0009-0001-8090-336X

Emily Conley
University of Minnesota Twin Cities College of Food Agricultural and Natural Resource Sciences

Zennah Kosgey
Kenya Agricultural & Livestock Research Organization

Ashenafi Gemechu Degete
Ethiopian Institute of Agricultural Research

Matthew Rouse
USDA-ARS CDL: USDA-ARS Cereal Disease Laboratory

James Anderson
University of Minnesota Twin Cities College of Food Agricultural and Natural Resource Sciences https://orcid.org/0000-0003-4655-6517

Research Article

Keywords: Khorasan wheat, Triticum turgidum ssp. turanicum, Stem rust, Ug99, Introgression

Posted Date: May 25th, 2023

DOI: https://doi.org/10.21203/rs.3.rs-2958205/v1

License: This work is licensed under a Creative Commons Attribution 4.0 International License. Read Full License

Abstract

The *Puccinia graminis* f. sp. *tritici* (*Pgt*) Ug99 race group presents a major challenge to global wheat production. Satisfying current and future demands hinges on the discovery of new sources of resistance. It is imperative that the durability and diversity of Ug99 resistance is improved by identifying and deploying novel resistance genes. Progenitor species and wild relatives of common wheat (*Triticum aestivum*) have proven to be rich sources of genetic diversity. The Khorasan wheat (*Triticum turgidum* ssp. *turanicum*) accession CItr 11390 displays adult plant resistance (APR) to Ug99 races. 121 BC_1F_5-derived recombinant inbred lines were developed from a cross between CItr 11390 and MN07098-6 to map and introgress resistance loci from CItr 11390. The population was evaluated in Kenya and Ethiopia in 2019 and 2020. Two APR QTL from CItr 11390 were detected in multiple environments. *QSr.umn-2A* is believed to be the APR gene *Sr63* on chromosome 2AL. *QSr.umn-6BL* was identified on 6BL upstream from *Sr11*. The distance from *Sr11* and lack of APR QTL reported on 6BL suggest *QSr.umn-6BL* is a novel locus. Additional QTL were mapped to chromosomes 1AS, 3AL, 3BL, 5AL, and 6BS in single environments. The population segregates for TKTTF seedling resistance conferred by *Sr7a* and a novel locus, *QSr.umn-5A.1*. The population consists of the first hexaploid wheat lines to pyramid *Sr7a*, *Sr57/Lr34/Yr18*, *Sr63*, and *QSr.umn-6BL*. This study is the first report of *Pgt* resistance QTL from Khorasan wheat, and it demonstrates the feasibility of simultaneously identifying and transferring resistance QTL from tetraploid to hexaploid wheat.

Key message

Multiple quantitative trait loci for adult plant resistance to *Pgt* races endemic to Kenya and Ethiopia were simultaneously identified and introgressed from tetraploid wheat accession CItr 11390 into common wheat.

Introduction

Worldwide, common wheat (*Triticum aestivum* L.) is the most widely grown crop with approximately 220 million hectares harvested annually. Global production of ~ 780 million tons of wheat provides 20% of the world's calories and protein (FAO 2022; Braun et al. 2010). In order to sustain this demand, wheat yields must increase 60% by 2050 (Godfray et al. 2010). Unfortunately, trends in wheat yields are inconsistent across major production regions and increasingly threatened by numerous biotic and abiotic factors (Grassini et al. 2013). Among these biotic factors is wheat stem rust caused by the fungus *Puccinia graminis* f. sp. *tritici* Eriks. and E. Henn. (*Pgt*).

Capable of destroying entire fields and reducing regional grain yields by up to 70% during epidemics, stem rust has been among the most damaging and feared diseases of wheat throughout history. Historical and archeological records of *Pgt* infection and stem rust epidemics extend across all major growing regions and date as far back as 3,300 BC (Kislev 1982; Roelfs 1985). However, outbreaks have greatly diminished since the early 20th century. Widespread deployment of genetic resistance to *Pgt*, disease control programs such as the Barberry Eradication Program in the United States, and the development of chemical fungicides effectively contained stem rust outbreaks to manageable levels throughout much of the 20th century (Singh et al. 2011).

During this period, stem rust disease resistance was largely qualitative in nature. Race-specific, all-stage resistance (ASR), also referred to as seedling resistance, was the cornerstone of stem rust resistance breeding efforts. The release of the hard red spring wheat variety 'Thatcher' by the University of Minnesota in 1934 was in direct response to a series of epidemics that afflicted the growing region in the preceding decades (Hayes et al. 1936). The rise of 'Thatcher' as the predominant variety grown throughout the Northern Great Plains of the United States and Canada into the 1960's was driven by a stem rust resistance package built around the ASR gene *Sr12* (Knott 2000). Beyond North America, stem rust was effectively controlled through the introgression and deployment of another ASR gene, *Sr31*, from the rye (*Secale cereale* L.) variety 'Petkus' beginning in the mid-1960s (McIntosh et al. 1995). Genetic control of stem rust using ASR genes such as *Sr12* and

Sr31 remained effective throughout much of the mid to late 20th century. Subsequently, breeding efforts and funding for fundamental and applied stem rust research were shifted towards the control of other pathogens (Singh et al. 2011).

Stem rust reemerged as a central topic of wheat research and breeding following the discovery of *Pgt* isolate Ug99 in Uganda in 1998 (Pretorius et al. 2000) and subsequent wheat stem rust epidemics in Kenya in 2004 and 2005. Later given the race designation TTKSK (Roelfs and Martens 1988), it was virulent to *Sr31* and several other resistance genes from common wheat and related species. Since the initial discovery of race TTKSK, the pathogen has undergone rapid genetic mutation and moved as far as South Africa, Yemen, and Iran (Terefe et al. 2018; Pretorius et al. 2012). Further migration of the Ug99 lineage of *Pgt* poses a major threat to global wheat production, as a study found that 85–90% of wheat varieties were susceptible to Ug99 (Singh et al. 2015).

The Ug99 lineage of stem rust is not the only threat to wheat production within Sub-Saharan Africa and beyond. Recent epidemics in Kenya and Ethiopia are attributed to races TKTTF, TTRTF, and JRCQC (Letta et al. 2013; Olivera et al. 2015; Patpour et al. 2020). The movement of these races outside the regions of their initial detection and the outbreaks they have caused highlight the need for constant pathogen monitoring, discovery of novel wheat stem rust resistance genes, and an emphasis on breeding for adult plant resistance.

Adult plant resistance (APR) is characterized by a reduction in both urediniospore size and production, and it is generally race nonspecific unlike like ASR (Stuthman et al. 2007). APR is believed to be a more durable form of resistance, as it is less prone to the boom and bust cycle associated with the successive deployment of individual ASR genes (Singh et al. 2011). Unfortunately, only six of the 63 named stem rust resistance genes confer APR: *Sr2* (McFadden 1930), *Sr55/ Lr67/ Yr46* (Herrera-Foessel et al. 2014), *Sr56* (Bansal et al. 2014), *Sr57/ Lr34/ Yr18* (Singh and Huerta-Espino 2003), *Sr58/ Lr46/ Yr29* (Martínez et al. 2001), and *Sr63* (Mago et al. 2022). Singh et al. (2011) hypothesized that pyramiding four to five APR genes could provide near immunity to *Pgt*. However, the expression and effectiveness of resistance genes is dependent on genetic background and environmental conditions (Kolmer 1996). Therefore, discovery and characterization of novel genes are essential to optimize gene pyramids and overcome the ability of *Pgt* to defeat deployed resistance genes.

Mapping and dissection of stem rust resistance genes has not been limited to hexaploid common wheat (AABBDD, 2n = 6x = 42). The progenitor species and wild relatives of common wheat have proven to be rich sources of diversity for numerous traits including stem rust resistance (Rowland and Kerber 1974). In total, stem rust resistance genes have been identified in 14 relatives of hexaploid wheat. The resistance genes identified in these relatives account for a majority of the genes that remain effective against the races of the Ug99 lineage (Singh et al. 2015). However, most of the introgressions are not used by breeding programs (Singh et al. 2015; Yu et al. 2014). Introgressions from species in the secondary and tertiary genes pools including *T. timopheevii* Zhuk. (AAGG, 2n = 4x = 28), *Secale cereale* L., and members of *Thinopyrum* and *Aegilops* are carried on Robertsonian translocations, which often harbor unfavorable alleles at genes influencing agronomic traits (Singh et al. 2011).

As opposed to members of the secondary and tertiary gene pools, the diploid and tetraploid progenitors of common wheat carry homologous chromosomes to those of common wheat capable of undergoing pairing and recombination, albeit with varying difficulty (Gill and Raupp 1987). In the case of *T. monococcum* (AA, 2n = 2x = 14), gene transfer is most often conducted through a bridge cross with durum wheat (*T. turgidum*, AABB, 2n = 4x = 28) (Sharma and Gill 1983). Direct hybridization with *T. monococcum* is complicated by the high rates of male and female sterility and lethality in F_1 hybrids (The 1973). However, direct introgression from *T. monococcum* is possible through extensive backcrossing as demonstrated by the transfer of *Sr21* and *Sr35* into hexaploid germplasm (The 1973; Zhang 2010). Introgressions from *Aegilops tauschii* (DD, 2n = 2x = 14) have historically been facilitated by first producing synthetic allohexaploid wheat through chromosome doubling of durum x *Ae. tauschii* F_1 hybrids. Direct crossing between *Ae. tauschii* and common wheat is a faster approach than developing synthetic allohexaploid lines despite the necessity of performing embryo

rescue, and it also avoids the disruption of adaptive allele combinations that have evolved in the A and B genomes (Gill and Raupp 1987). Olson et al. (2013a, b) demonstrated the feasibility of direct crossing with *Ae. tauschii* by simultaneously mapping and introgressing stem rust resistance loci *SrTA1662*, *Sr10171*, and *Sr10187* in populations developed after two rounds of backcrossing to *T. aestivum* recurrent parents.

Direct introgression of stem rust resistance genes from emmer and durum wheat (AABB, 2n = 4x = 28) is well documented and does not require specialized techniques (Lanning et al 2008; Laugerotte et al. 2022). Examples include *Sr2* introgressed from *T. turgidum* ssp. *dicoccum* variety 'Yaroslav' (McFadden 1930), *Sr11* from *T. turgidum* ssp. *durum* variety 'Gaza' (Green et al. 1960), *Sr12* from *T. turgidum* ssp. *durum* variety 'Iumillo' (Knott 2000), and *Sr13* and *Sr14* from *T. turgidum* ssp. *dicoccum* variety 'Khapli' (Knott 1962). Similar to the approach described by Olson et al., (2013a, b), QTL influencing yield component traits and *Yr53*, a gene for stripe rust (caused by *P. striiformis* f. sp. *tritici*) resistance, were simultaneously mapped and transferred into common wheat from tetraploid wheat accessions (Kalous et al. 2015; Xu et al. 2013).

The primary objective of this study was to identify the underlying loci conferring APR to Ug99 lineage races of *Pgt* in the Khorasan wheat accession (*Triticum turgidum* ssp. *turanicum*) CItr 11390 ('Sun Ray'). In an effort to simultaneously transfer these loci to hexaploid wheat lines while reducing the effects of poor agronomic alleles from CItr 11390 and recovering euploid progeny, a BC_1F_5-derived recombinant inbred line (RIL) population was developed.

Materials and methods

Plant materials

A mapping population of 121 BC_1F_5-derived RILs was developed from an interspecific cross between tetraploid accession CItr 11390 and the hexaploid recurrent parent MN07098-6. CItr 11390 ('Sun Ray') is a Khorasan wheat (*Triticum turgidum* ssp. *turanicum*) accession of unknown improvement status within the USDA National Small Grains Collection. MN07098-6 (SD3696/MN97803-3BS) is a hard red spring wheat breeding line susceptible to the Ug99 lineage from the University of Minnesota. The population was developed from a single BC_1F_1 plant. The BC_1F_2 progeny were advanced in the greenhouse using the single seed descent method, and a seed increase was conducted at the BC_1F_5 generation to obtain enough seed for field experiments.

Seedling stage stem rust phenotyping

The RILs and parents were evaluated for seedling infection types to *Pgt* races TTKSK (isolate 04KEN156/04; Ug99), TTKTT (isolate 14KEN58-1; Ug99 with *Sr24* and *SrTmp* virulence), TKTTF (isolate 13ETH18-1), and TTRTF (isolate 14GEO189-1) at the United States Department of Agriculture – Agricultural Research Service (USDA-ARS) Cereal Disease Lab in Saint Paul, Minnesota. Inoculation and phenotyping procedures were conducted as described by Rouse et al. (2011). All lines were evaluated in four replications. Infection types (ITs) were recorded on a 0–4 scale described by Stakman et al. (1962). IT scores were converted to a linearized scale for QTL mapping according to Gao et al. (2016).

Field-based stem rust evaluation

The $BC_1F_{5:6}$ and $BC_1F_{5:7}$ populations, as well as the parents, were evaluated for field response to African *Pgt* races during the off-seasons (January – May) of 2019 and 2020 in Njoro, Kenya (hereafter referred to as Ken19 and Ken20, respectively) and Debre Zeit, Ethiopia (hereafter referred to as Eth19 and Eth20, respectively).

In all environments, the lines were grown in a randomized complete block design with two replications. In Kenya, each line was grown in two 0.7 m rows spaced 0.3 m apart. The susceptible check CItr 6255 ('Red Bobs') was planted after every fifty entries. Twin spreader rows consisting of susceptible varieties 'Cacucke', 'Eagle 10', 'Robin', and six CIMMYT experimental lines were grown alongside and between each plot. Additionally, a border of spreader rows encompassed the nursery. Starting at the booting growth stage through heading (Zadok's growth stage 37–60), spreader rows were inoculated with a

bulk inoculum of locally collected urediniospores. *Pgt* races TTKSK, TTKST, TTKTK, and TTKTT were among the races present in the Kenya nurseries (Mago et al. 2022). In Ethiopia, lines were grown in 1.0 m double rows flanked by spreader rows consisting of susceptible varieties 'Arendeto', 'Digalu', 'Local Red', 'Morocco', and 'PBW343' (Kosgey et al. 2021). Spreader rows were inoculated at Zadok's growth stages 37–60 using bulk of locally collected urediniospores.

Stem rust severity was assessed once spreaders and the check line CItr 6255 reached 50% severity in both Kenya and Ethiopia. Stem rust severity was scored on a whole plot basis using the modified Cobb scale of 0 to 100%, where 0 is equal to complete immunity or absence of infection symptoms and 100% is equal to complete susceptibility (Peterson et al., 1948). Infection response (IR) was recorded based on pustule size and prevalence of chlorosis and necrosis. Four classifications were assigned for IR: S, susceptible; MS, moderately susceptible; MR, moderately resistant; and R, resistant (Roelfs et al. 1992). Lines with heterogeneous infection responses were denoted using a hyphen (e.g. MS-MR) with the most prevalent IR category listed first. Linearized infection response (LIR) and coefficient of infection (CI) were calculated from the field observations using a custom R script (Gao et al. 2016). LIR is infection response scaled from 0 to 1.0. CI was then calculated as the product of LIR and severity (Stubbs et al. 1986). Two observations were recorded in both years in Kenya, while three observations were made in Ethiopia. However, only the CI value from the final observation in each environment was considered during data analysis and QTL mapping.

Genotyping

Single nucleotide polymorphism markers (SNPs) were called using genotyping-by-sequencing (GBS; Elshire et al. 2011). DNA was extracted from juvenile leaves collected from the parents and $BC_1F_{5:6}$ RILs using BioSprint 96 DNA Plant Kits (QIAGEN, Hilden, Germany). Extracted DNA was quantified using Quant-iT PicoGreen dsDNA assay kits (Invitrogen, Waltham, Massachusetts, USA) and normalized to 20ng/µL. GBS libraries were constructed using a two-enzyme approach as described by Poland et al. (2012) with two modifications: 1) two unique barcodes were ligated to each sample in an effort to reduce sequencing bias of certain barcodes and 2) barcode and common adapter concentrations were increased to 0.1 µM and 50 µM, respectively. Two 64-plex libraries were generated including four biological replicates of parent MN07098-6 and three biological replicates of parent CItr 11390. Each library was sequenced on one Illumina HiSeq 2000 lane to produce single-end 100 bp reads.

Marker calling, filtering, imputation, and distortion

Raw sequencing reads were demultiplexed using Sabre (https://github.com/najoshi/sabre). Adapters and low quality bases (Q < 30) were trimmed using Cutadapt (Martin 2011). Trimmed reads were aligned to the *T. aestivum* cv. Chinese Spring reference assembly, RefSeq v2.1 (Zhu et al. 2021) using the BWA-MEM algorithm with default parameters (Li 2013). Aligned reads were filtered (MAPQ < 40) and sorted with SAMtools, and SNP calling was done with BCFtools (Li 2011; Li et al. 2009). Genotypes within a site were set to missing data based on read depth (DP < 3). Sites with ≥ 20% missing data and QUAL < 20 were then discarded as well as monomorphic and multiallelic sites. Sites were further filtered by removing those with a minor allele frequency (MAF) < 40% or heterozygosity > 10%. Missing marker data were imputed in TASSEL 5 using LD-kNNi, an imputation method based on the *k*-nearest neighbor algorithm (Bradbury et al. 2007; Money et al. 2015). Genotypes were converted from a nucleotide-based format to a parent-based format, and consensus genotypes were called for both parents from the replicated samples using the GenosToABHPlugin in TASSEL 5 (Bradbury et al. 2007).

Further marker analysis and filtering was performed in R using the 'qtl' and 'ASMap' packages (Broman et al. 2003; R Core Team 2022; Taylor and Butler 2017). Redundant markers with identical genotype patterns across all individuals were identified, and all but one representative marker were removed from the data set. Using the filtered dataset, all pairwise marker similarities were calculated among the individuals. Individuals with identical genotypes at ≥ 95% markers were identified, and the line with a greater amount of missing data among the pair was removed from analysis. Lastly, markers were tested for segregation distortion.

Molecular marker screening

The parents and population were screened with a series of markers previously described as linked to resistance loci: *Sr7a*, *Sr11*, *Sr12*, *Sr13*, *Sr21*, *Sr38/Lr37/Yr17*, *Sr63*, *Sr8155B1*, and *SrTm4* (Table 1). Additionally, shortly after population development concluded, MN07098-6 was found to be heterogeneous for *Sr57/Lr34/Yr18* on chromosome 7D. The plant used for the backcross was not the selfed progeny of the original MN07098-6 crossing parent. Therefore, the lines used for the initial and backcross were potentially near-isogenic for *Sr57/Lr34/Yr18*. The population was screened for *Sr57/Lr34/Yr18* to determine if the population was segregating at this locus using a perfect marker (Table 1).

Aneuploidy and chromosomal deletion detection

In silico detection of aneuploidy and chromosomal deletions among the progeny lines was conducted using the GBS data and a method adapted from Singh et al. (2020). MN07098-6 and CItr 11390 were used as euploid allohexaploid and allotetraploid controls, respectively. Each chromosome was divided in 100 Mb bins with a sliding window step size of 50 Mb. Bins < 50 Mb in length at the end of chromosomes were discarded as they nested completely within another bin. BEDtools multicov (Quinlan and Hall 2010) was used to count the number of reads uniquely aligned within each bin. Counts were normalized across the genome for all bins and individuals to remove bias due to differential sequencing. Karyotypes for each sample were plotted using base R functions and the 'chromPlot' package (Oróstica and Verdugo 2016; R Core Team 2022). Bins were assigned a copy number based on normalized values. Due to artifacts in the assembly leading to a small number of reads aligning to D genome chromosomes for CItr 11390, the mean normalized value across all bins deviated slightly from one. Therefore, the upper bin value limit for each copy number was determined using the following equation:

$$bin_{max} = \frac{copynumber * \mu}{2} + 2\sigma$$

where μ and σ are the mean normalized values and standard deviation across all bins, respectively. Karyotype plots were visually assessed to detect chromosomal deletions and aneuploidy. Individuals with signatures for any form of aneuploidy involving chromosomes of either the A or B genome were not included in genetic and phenotypic analysis. Additionally, RILs with all forms of aneuploidy or deletions other than monosomy in the D genome were excluding from further analysis. RILs with monosomy affecting a single D genome chromosome were included in initial data analysis as there is representation of all 21 chromosomes.

Linkage map construction

Linkage map construction was performed in R using the MSTmap algorithm implemented in the package 'ASMap' (R Core Team 2022; Taylor and Butler 2017; Wu et al. 2008). Due to the population being developed from a single BC_1F_1 plant, it was treated as a self-pollinated RIL population despite the generation of backcrossing. Linkage groups were independently constructed for each chromosome based on the physical positions assigned to the GBS markers. Map construction and marker ordering was conducted using the Kosambi mapping function and a significance threshold for marker clustering of $p = 10^{-6}$ (Kosambi 1943). Final marker order was set by jittering the positions of markers mapped to the same position.

Data analysis

Seedling-stage stem rust resistance

Mean values calculated from the converted infection type scores across the four replications for *Pgt* races observed to have variable virulence to the parents were used for analysis and QTL mapping. Lines with a linearized score of < 6 were considered resistant whereas those with scores ≥ 6 were considered susceptible. A chi-square (χ^2) test was conducted to determine the genetic architecture of resistance to the screened *Pgt* races within the population.

Field-based stem rust

The population was determined to be segregating for *Sr57/Lr34/Yr18*. To determine the significance of the effects of *Sr57/Lr34/Yr18* and ploidy on stem rust CI, mixed linear models were fit in R using the '*lme4*' package (Bates et al. 2015). *Sr57/Lr34/Yr18*, ploidy state, and environments treated as fixed effects. Genotypes, genotype-environment interactions, and blocks within environments were treated as random effects. Backwards elimination of all effects in the across-environment model was performed using the '*lmerTest*' package in R (Kuznetsova et al. 2017). Significance values for the fixed and random effects were calculated based on Sattethwaite's approximation and likelihood ratio tests, respectively.

The interaction between genotype and environment was determined to be significant, which warranted the separate analysis of each environment. CI values within environments were then adjusted for the effect of *Sr57/Lr34/Yr18* by fitting mixed linear models for each of the four environments separately. *Sr57/Lr34/Yr18* was significant in the across-environment model, while ploidy was determined to be insignificant. Therefore, *Sr57/Lr34/Yr18* was the only fixed effect retained in the individual environment models. Genotype and block were included as random effects.

In addition to visual inspection of diagnostic plots for each single environment model, residuals were tested for normality and homogeneity with Sharpiro-Wilk and Levene's tests, respectively. If necessary, data transformation was performed if assumptions of normality and residual homogeneity were violated. Log and square root transformations were tested for each environment. Additionally, an arcsine transformation of the Eth20 data was tested after dividing the data by 100. The model selection approach above was repeated to assess the effectiveness of each transformation. Coefficients from the selected models were extracted to correct phenotypic values for the effect of *Sr57/Lr34/Yr18*. Pearson correlation coefficients between environments were calculated in R using the adjusted datasets.

QTL Mapping

QTL detection within individual environments was conducted using multiple QTL mapping (MQM) in R using the '*qtl*' package (Broman et al. 2003). Multiple QTL mapping was conducted using an automated forward/backward analysis, and the final models were selected based on penalized LOD score (pLOD; Manichaikul et al. 2009). First, a single locus model was fitted for each environment and race with segregating resistance using multiple imputation and the scanone function. A 95% significance threshold for each single locus scan was determined by 1000 permutations across the entire genome. Significant markers ($\alpha = 0.05$) from the single locus models were used as the initial set of cofactors for MQM analysis. Next, a two-dimensional genome scan was performed with 1000 permutations to calculate the threshold for significant LOD scores ($\alpha = 0.05$) described by Broman et al. (2003) using the scantwo function. These thresholds were then used to calculate the pLOD scores to be used for multiple QTL mapping. Using the loci detected by single-QTL scans and the calculated pLOD thresholds, Multiple QTL models with maximal pLOD scores were selected and refined using the stepwiseqtl command and multiple imputation. Within the stepwiseqtl function, forward selection was allowed to proceed with a maximum of 10 QTL. The reported LOD support intervals, reported as 95% Bayes credible intervals, were calculated using the command bayesint.

Assessment of QTL interactions and combinations

All pairwise QTL x QTL interactions were simultaneously tested during multiple QTL model selection using stepwiseqtl, and models were refined in the event of a significant interaction between QTL. Significance and percent of phenotypic variance explained of the final models including interactions was determined in R using the fitql command from the 'qtl' package.

Mean CI values of RILs carrying all combinations of QTL detected in multiple environments, as well as *Sr57/Lr34/Yr18*, were compared within each environments. Mean CI values of each class of RILs were calculated based on the allele at the peak marker of the QTL using the unadjusted and untransformed data from each environment. Tukey's HSD tests were performed to determine whether the means of each class of RIL were significantly different within each environment.

Molecular marker development

PCR Allele Competitive Extension (PACE™) SNP genotyping assays (3CR Bioscience, Harlow, UK) were developed for novel QTL detected in multiple environments. Primers were designed at GBS SNPs throughout the LOD intervals. Primers targeting resistance alleles were labelled with the HEX fluorophore, and those for susceptible alleles were labelled with the FAM fluorophore. Each PACE™ assay mix contained 60 µL HEX-labeled primer (100 µM), 60 µL FAM-labeled primer (100 µM), 120 µL common primer (100 µM), and 230 µL molecular-grade water (Sigma Cat. No. 4502). For each assay, genotyping was conducted using standard conditions for PACE. 8 µL reactions consisted of 2 µL template DNA (20 ng/µL), 0.11 µL assay mix, 4 µL 2x PACE™ master mix, and 1.89 µL molecular grade water. Genotyping was performed on a Roche Lightcycler® 480 (Roche Diagnostics, Indianapolis, IN, USA) using the following reaction conditions: hot-start activation at 95°C for 15 minutes, 10 touchdown cycles at 94°C for 20 seconds, touchdown at 61°C for 1 minute with a 0.6°C reduction per cycle until a secondary target of 55°C, and 48 cycles at 94°C for 20 seconds followed by 55°C for 1 minute/cycle. An endpoint read was taken following a 2-minute cooldown cycle at 37°C. Alleles were called using the Roche Lightcycler® 480 Endpoint Genotyping Software Module.

Results

Genotyping and Aneuploid Detection

Genotyping-by-sequencing (GBS) resulted in a total of 269,278,521 uniquely mapped reads across all samples. The distribution of read counts per sample was relatively normally distributed, and the median number of reads per sample was ~ 2.2 million (Fig. S1A). Total read counts were first normalized across all samples. Counts in each bin were then normalized by the median count for each bin across all samples. As expected, the distribution of normalized read counts per bin had a normal distribution (Fig. S1B). Small shoulder peaks were observed in the distribution centered around 0, 0.5, and 2.0, which represent deleted, monosomic, and duplicated bins, respectively. Over 98% of bins had a normalized read count around 1.0, representative of the disomic state.

The analysis accurately assigned a copy number of 0 to all D genome chromosomes of the tetraploid parent, Cltr 11390, while all 21 chromosomes in MN07098-6 were determined to be disomic and fully intact as expected (Fig. 1). Of the 121 RILs, 30 were determined to be aneuploids (Fig. S2). Of the 30 aneuploid RILs, 24 had an abnormality with chromosomes in homoeologous groups 4 or 6, with 18 possessing chromosome 6D abnormalities (Table S1). The most common form of aneuploidy was monosomy (15 out of 30 lines). Notes made in observation nurseries in 2019 in Saint Paul, Minnesota and Crookston, Minnesota corroborate the *in silico* analysis. Several of the RILs identified as aneuploids were noted in both locations to have poor vigor, short stature, and/or late maturity. The 30 RILs identified as aneuploids, as well as one RIL of a pair with > 95% identical SNPs, were initially retained during variant calling. However, the 16 RILs with forms of aneuploidy or deletions involving the A or B genome, as well as 1 euploid RIL of the pair found to have > 95% identical SNPs, were removed during SNP filtering. The remaining 14 aneuploid RILs (11 M6D and 3 M4D) were included in phenotypic data analysis to determine whether monosomy involving either chromosome had a significant effect on stem rust infection.

Linkage map construction

After filtering, 2,287 SNPs were obtained from GBS across the A and B genomes. No SNPs in the D genome remained after filtering as expected. In addition to the GBS SNPs, markers linked to previously mapped stem rust resistance genes were used for linkage mapping. Of the molecular markers assayed, those linked to *Sr7a*, *Sr11*, *Sr63*, and *Sr8155B1* were polymorphic between the parents and added to the GBS marker dataset (Table 1). Additionally, the population was segregating for *Sr57/Lr34/Yr18*. However, as no GBS SNPs were retained on chromosome 7D after filtering, *Sr57/Lr34/Yr18* was not included in linkage mapping.

Table 1
Molecular marker assays for known stem rust resistance genes

			Parent allele		
Gene	Chromosome	Marker	MN07098-6	Cltr 11390	Reference
Sr7a	4AL	KASP_IWB12146 KASP_IWB47019 KASP_IWB68386	G[b]	A[a]	Bajgain et al. 2015a; Olivera et al. 2022
Sr11	6BL	KASP_IWB72471	T[a]	G[b]	Nirmala et al. 2016
Sr12	3BL	NB-LRR3	G[b]	G[b]	Hiebert et al. 2016
Sr13	6AL	Sr13R/S_SNP	A[a]	Null	maswheat.ucdavis.edu/protocols/Sr13
Sr21	2AL	Sr21TRYF5R5	Null	Null	Chen et al. 2018
Sr38/Lr37/Yr17	2NS:2AS	Lr37-Yr17-Sr38_GBG-KASP	A[a]	A[a]	Helguera et al. 2003; Mustahsan 2022
Sr57/Lr34/Yr18	7DS	wMAS000003	T/A[c]	A[a]	maswheat.ucdavis.edu/protocols/Lr34
Sr63	2AL	KASP_IWB32429	T[a]	G[b]	Mago et al. 2022
Sr8155B1	6AS	KASP_IWB10558	A[a]	G[b]	Nirmala et al. 2017
SrTm4	2AL	BQ421276 DR732348	Null	Null	Briggs et al. 2015

[a] Reportedly predictive of susceptibility

[b] Reportedly predictive of resistance

[c] MN07098-6 is heterogeneous for *Sr57/Lr34/Yr18*

The 2,291 GBS and molecular markers used for linkage mapping were assigned to 21 linkage groups representing the 14 chromosomes of the A and B genomes. Chromosomes 1B, 2A, 2B, 3B, 5A, 5B, and 6A were represented by a single linkage group, while the other seven chromosomes were split into two linkage groups each. Following marker ordering, markers with identical genotypes were identified and all but one representative marker for each group of markers were removed from the map. The final map consisted of 1,212 markers with a total length of 1,230.7 cM and an average spacing of ~ 1.0 cM between markers.

Seedling-stage disease evaluation

Parental infection types to the four *Pgt* races screened are shown in Table 2. MN07098-6 and Cltr 11390 were both susceptible at the seedling stage (IT = 33 + c to 3+) to the two Ug99 lineage races screened (TTKSK and TTKTT). The results of the TTKTT screen were unexpected, as Cltr 11390 was found to carry the allele at KASP_IWB10558 reported to be predictive of resistance provided by *Sr8155B1* (Nirmala et al. 2017). Note that Nirmala et al. (2017) reported the same isolate of TTKTT used in this study, 14KEN58-1, to be avirulent to *Sr8155B1* with infection type '0;'. However, the same study reported the 04KEN156/04 isolate to be virulent to *Sr8155B1* with infection type '3+'.

Initial inspection of the data indicated CItr 11390 was moderately resistant to TTRTF (IT = 2). However, analysis of the RILs found only four resistant lines (mean linearized IT < 6) to 100 susceptible lines (mean linearized IT ≥ 6). Additionally, the upper bound of the 95% confidence interval for all four RILs with a mean linearized IT < 6, was greater than the threshold for resistance (Fig. S4). Therefore, TTRTF was not included in QTL mapping.

Table 2
Isolate designation, origin, parental infection type, and virulence phenotype of *Puccinia graminis* f. sp. *tritici* races used to evaluate seedling resistance in the population.

Race	Isolate	Origin	MN07098-6	CItr 11390
TTKSK	04KEN156/04	Kenya	3+	3+
TTKTT	14KEN58-1	Kenya	3+	33 + c
TKTTF	13ETH18-1	Ethiopia	12-	3+
TTRTF	14GEO189-1	Georgia	3-	2

Variation between the parents for seedling resistance to TKTTF was observed. MN07098-6 had a mean linearized IT of 2.7. This finding was as expected given MN07098-6 carries *Sr7a*, a gene known to confer resistance to TKTTF (Edae et al. 2018; Turner et al. 2016). CItr 11390 was susceptible to TKTTF with a mean linearized IT of 8.8 (Fig. S4). The susceptibility of CItr 11390 was notable as it was found to carry the allele reported to be predictive of resistance at KASP_IWB72471, a marker linked to *Sr11* (Nirmala et al. 2016). Analysis of the RILs found an approximately 1:1 segregation ratio of resistance with 57 resistant RILs and 47 susceptible RILs supporting the hypothesis that resistance to TKTTF in the population is provided by a single resistance gene (Table 3). A chi-square test resulted in the acceptance of the null hypothesis that resistance to TKTTF in the population is monogenic ($\chi^2 = 1.0$, $p > 0.32$; Table 3).

Table 3
Chi-square test for segregation of stem rust reaction to TKTTF in the 15xR012 population

Race	No. of resistant RILs (IT ≤ 6)	No. of susceptible RILs (IT > 6)	Observed segregation	χ^2	Number of expected genes
TKTTF	57	47	1:1	(1, N = 104) = 1.0, $p > 0.33$	1 gene

Linkage mapping for seedling resistance to TKTTF

MQM analysis was performed to validate the effectiveness of *Sr7a* against TKTTF. A large-effect QTL was detected on 4AL (LOD = 29.2; $R^2 = 69.8\%$; Table 4; Fig. S5) that colocated with the *Sr7a*-linked KASP markers screened on the population. Unexpectedly, a second resistance loci was retained in the final model on the long arm of chromosome 5A (LOD = 29.2; $R^2 = 4.6\%$; Table 4; Fig. S5). Like *Sr7a*, the resistance allele at this locus is donated by the hexaploid parent, MN07098-6.

Table 4
Quantitative trait loci (QTL) for seedling resistance to TKTTF in the 15xR012 population detected by multiple QTL mapping (MQM). All QTL are significant at α < 0.05

Race	QTL[a]	Chr	Flanking markers[b]		Pos (cM)	LOD[c]	$R^{2\,d}$	Add[e]
			Left	Right				
TKTTF	*QSr.umn-4A*	4AL	S4A_720268179	S4A_728943337	7.0	29.2	69.8	2.7
	QSr.umn-5A.1	5AL	S5A_553400727	S5A_605408042	109.2	3.6	4.6	0.6

[a] Named according to McIntosh et al. (2020)

[b] 95% Bayes credible interval

[c] Peak logarithm of odds

[d] Phenotypic variance explained

[e] Estimated additive effect of QTL; negative value indicates that the allele donor is CItr 11390

Field-based disease evaluation

CItr 11390 displayed high levels of resistance in Kenya in both 2019 and 2020, but the accession was far less resistant in both Ethiopian nurseries (Table 5). MN07098-6 was susceptible in all four environments with mean severity ranging from 60 to 75% within individual environments (Table S2). Disease pressure was especially high in Ethiopia in 2019, and scoring was conducted later than the optimal window. Both parents and the RIL population displayed completely susceptible infection responses and almost no variation in severity was observed (Tables S2 and S3). Raw stem rust CI distributions were continuous and positively-skewed in Kenya in 2019 and 2020 (Fig. 2). Visual assessment of a Q-Q plot indicated the Eth20 data had a slightly negative skew. Residuals for Ken19 and Ken20 were in violation of the assumption of normality based on Shapiro-Wilk tests ($p < 0.05$). Only the residuals for Ken20 were heteroscedastic based on Levene's test ($p < 0.05$).

Table 5
Mean stem rust coefficient of infection values, standard deviations, and ranges in the 15xR012 mapping population in four field environments.

Environments[a]	Parent mean coefficient of infection		Population	
	CItr 11390	MN07098-6	Mean ± SD	Range
Eth19	60.0	60.0	58.3 ± 3.1	45.0–60.0
Eth20	40.0	65.0	59.2 ± 12.3	24.0–80.0
Ken19	2.5	60.0	35.5 ± 22.4	2.0–90.0
Ken20	8.3	75.0	41.0 ± 21.8	8.0-100

[a] Eth19 = Debre Zeit, Ethiopia 2019; Eth20 = Debre Zeit, Ethiopia 2020; Ken19 = Njoro, Kenya 2019; Ken20 = Njoro, Kenya 2020

Square root transformation of the Ken19 values resulted in the restoration of normality. Square root transformation of the Ken20 values also resulted in the restoration of normality and homoscedasticity, as well as marked improvement in the Q-Q plot. Therefore, the transformed data were used for Ken19 and Ken20.The Eth20 data were divided by 100 followed by an arcsine transformation. While a Shapiro-Wilk test indicated that the transformed data were normally distributed, little to no differences were viewed between the Q-Q plots of the untransformed and transformed data fitted with the same model. Given these observation, as well as the homogeneity of the untransformed residuals and the increased difficulty of

interpreting QTL mapping results from transformed datasets, the untransformed data from Eth20 were used for further analyses.

The 15xR012 population was found to segregate for *Sr57/Lr34/Yr18* due to near-isogenic MN07098-6 lines being used for population development. *Sr57/Lr34/Yr18* was found to have a significant effect on CI in a mixed model using the data from all environments. Due to a complete absence of additional markers linked to *Sr57/Lr34/Yr18* on chromosome 7D, the effect of the gene was adjusted using mixed models fitted within each environment. The estimated marginal means of CI for the resistance allele at *Sr57/Lr34/Yr18* was 30.0%, 46.5%, and 11.1% lower than the susceptible allele in Ken19, Ken20, and Eth20, respectively. After adjustment, mean CI increased slightly in Ken19, Ken20, and Eth20 (Fig. 3). Adjusted CI values of the RILs between all environments were significantly correlated (Table 6).

Table 6
Pearson correlation coefficients (*r*) of adjusted stem rust coefficient of infection values observed in the 15xR012 population in four field environments in Ethiopia and Kenya in 2019 and 2020

	Eth19	Eth20	Ken19	Ken20
Eth20	0.37***			
Ken19	0.23*	0.33***		
Ken20	0.20*	0.39***	0.66***	
Eth19 = Debre Zeit, Ethiopia 2019; Eth20 = Debre Zeit, Ethiopia 2020; Ken19 = Njoro, Kenya 2019; Ken20 = Njoro, Kenya 2020				
* Correlation is significant at α < 0.05				
** Correlation is significant at α < 0.01				
*** Correlation is significant at α < 0.001				

Linkage mapping of stem rust resistance

Multiple QTL mapping (MQM) detected significant QTL associated with APR in three of the four African nurseries (Table 7; Fig. S6). No QTL were detected in Eth19. In total, seven QTL were detected in at least one environment. The LOD scores of the detected QTL ranged from 3.3 to 20.9. Of the seven QTL, two were detected in more than one environment. *QSr.umn-6BL* was detected in Eth20 and Ken20. It explained 10.2% of the observed phenotypic variation in Eth20 and 10.5% in Ken20. While *QSr.umn-6BL* was not retained in the multiple QTL model, it was detected by single-QTL and two dimensional genome scans (Table S4).

The second multi-environment QTL, *QSr.umn-2A*, was detected in Kenya in 2019 and 2020. *QSr.umn-2A* explained 42.8% of the phenotypic variation in 2019 and 44.6% of variation in 2020. The peaks for *QSr.umn-2A* were sharply centered around KASP marker Sr63_IWB32429 for Ken19 and Ken20, indicating that *QSr.umn-2A* could be *Sr63*.

QSr.umn-2A and *QSr.umn-6BL* were each contributed by the tetraploid parent, CItr 11390. The five other QTL were only detected in a single environment and explained 5.0-21.5% of the observed phenotypic variation within their respective environments. Notably, the interval of *QSr.umn-5A.2* co-located with the TKTTF ASR-associated QTL, *QSr.umn-5A.1*. The resistance allele was contributed by MN07098-6 at both *QSr.umn-5A.1* and *QSr.umn-5A.2*. Of the remaining single-environment QTL, three were contributed by MN07098-6 and one was contributed by CItr 11390 (Table 7).

Table 7
Quantitative trait loci (QTL) for field-based stem rust resistance in the 15xR012 population detected by multiple QTL mapping (MQM). All QTL are significant at $\alpha < 0.05$

Environment[a]	QTL[b]	Chr	Flanking markers[c]		Pos (cM)	LOD[d]	R^{2} [e]	Add[f]
			Left	Right				
Eth20	*QSr.umn-1A*	1AS	S1A_5914856	S1A_15479164	10.0	6.4	21.5	1.6
	QSr.umn-6BL	6BL	S6B_467576061	S6B_651836748	13.0	3.3	10.2	-1.1
Ken19	*QSr.umn-2A*	2AL	S2A_681051011	S2A_702504398	139.0	14.1	42.8	-0.8[g]
	QSr.umn-5A.2	5AL	S5A_488255473	S5A_659345920	77.0	4.2	10.1	0.4[g]
Ken20	*QSr.umn-2A*	2AL	S2A_681051011	Sr63_IWB32429	136.0	20.9	44.6	-0.67[g]
	QSr.umn-3A	3AL	S3A_603255953	S3A_654993190	105.0	3.6	5.0	0.22[g]
	QSr.umn-3B	3BL	S3B_429246336	S3B_490054756	33.1	6.6	10.0	0.32[g]
	QSr.umn-6BS	6BS	S6B_17383541	S6B_36319780	16.7	10.0	16.2	-0.22[g]
	QSr.umn-6BL	6BL	S6B_572334604	S6B_602404199	31.7	6.9	10.5	-0.31[g]

[a] Eth20 = Debre Zeit, Ethiopia 2020; Ken19 = Njoro, Kenya 2019; Ken20 = Njoro, Kenya 2020

[b] Named according to McIntosh et al. (2020)

[c] 95% Bayes credible interval

[d] Peak logarithm of odds

[e] Phenotypic variance explained

[f] Estimated additive effect of QTL; negative value indicates that the allele donor is CItr 11390

[g] Value is reported as the square root of coefficient of infection

Assessment of QTL interactions and combinations

Tests for epistasis while fitting the multiple QTL models detected one significant interaction within Ken20. The interaction between *QSr.umn-2A* and *QSr.umn-6BS* explained 10.9% of the observed phenotypic variation in Ken20 ($p < 0.001$). The resistance allele was donated by CItr 11390 at both QTL. The mean CI of lines carrying only the resistance allele at *QSr.umn-2A* was significantly lower than those carrying only the resistance allele at *QSr.umn-6BS*. However, the difference in mean CI between lines only carrying the resistance allele at *QSr.umn-2A* and those carrying resistance alleles at both loci was not significant (Fig. 4a, 4b, Table S5).

QSr.umn-6BL was detected in two environments by MQM while *QSr.umn-2A* was detected in Kenya in both years. In addition to the detected QTL, the effect of *Sr57/Lr34/Yr18* was significant on CI in all three environments. Multiple RILs in each of the eight possible combinations of these three loci were found among the population: No QTL, *Sr57*, *QSr.umn-2A* (hereafter referred to as *Sr63*), *QSr.umn-6BL*, *Sr57* + *Sr63*, *Sr57* + *QSr.umn-6BL*, *Sr63* + *QSr.umn-6BL*, and *Sr57* + *Sr63* + *QSr.umn-6B*.

Significant differences were observed among the allelic combinations in all environments. In Eth20, the mean CI of RILs carrying a single gene was lower than lines lacking all three genes. However, these differences were not significant. All

combinations of two or all three resistance alleles resulted in a significant reduction in mean CI (Fig. 5, Table S6). The mean unadjusted CI of lines carrying all three genes was 52.0 compared to 69.3 for lines lacking all three genes.

Within the Kenyan environments, many of the pairwise comparisons were not statistically significant. However, this is possibly due to the low sample size of RILs constituting each of the eight groups of gene combinations (Fig. 5, Table S6). Despite this finding, additive relationships were observed among the three genes. The mean unadjusted CI values of RILs carrying no resistance alleles at the three loci (Ken19: 61.6; Ken20: 66.9) were over three times greater than those carrying the resistance allele each of the three genes in both environments (Ken19: 18.2; Ken20: 18.5).

Molecular marker development

PACE ™ SNP genotyping assays were developed for *QSr.umn-6BL* at loci approximately flanking the QTL peaks detected by single-QTL genome scans in Eth20, Ken19, and Ken20. The markers with the clearest results were determined to be at loci correspond to positions 655,795,233 and 675,524,532 on chromosome 6B of RefSeq v2.1 assembly (Table S7). Genotyping calls for both assays were found to be concordant with the GBS markers (Table S8).

Discussion

The discovery and deployment of new stem rust resistance genes from diverse sources is vital to the sustained production of wheat on both regional and global scales. Since the initial discovery of *Pgt* race TTKSK (Ug99) in Uganda in 1998 (Pretorius et al. 2000), an additional fourteen variants have been identified with unique virulence profiles. The Ug99 race group has moved well beyond Uganda, with variants detected in fourteen countries spanning a geographic range from Iraq to South Africa (Terefe et al. 2018; Pretorius et al. 2012). The Ug99 race group is not the only threat posed by *Pgt*. The need for continued monitoring and resistance breeding for other *Pgt* races is evidenced by the detection and geographic expansion of races TKTTF, TTRTF, JRCQC, and TTTTF, some of which are virulent to widely deployed resistance genes including *SrTmp* and *Sr13b* (Letta et al. 2013; Olivera et al. 2015; Patpour et al. 2020).

The challenge of discovering novel sources of stem rust resistance for wheat is aided by the rich gene pools available to wheat breeders and pathologists (Rowland and Kerber 1974). However, as demonstrated by this study, the integration of ancestral wheat species and other members of the *Aegilops* tribe into downstream breeding is not a straightforward process (Leigh et al. 2022). Of the 121 BC_1F5-derived RILs developed, 30 were aneuploids and removed from further phenotypic analysis and QTL mapping (Table S1).

Stem rust infection was much greater in both Ethiopian environments than either Kenyan environment. It is possible this difference was driven by the warmer environment in Ethiopia, as temperature has been found to significantly impact the effectiveness of ASR and APR genes (Chen et al. 2018; Gao et al. 2019; McIntosh et al. 1995; Zhang et al. 2017). Alternatively, the differences could be driven by the presence of additional races in Ethiopia. Races TRTTF and JRCQC have previously been identified from isolates collected in the Debre Zeit nursery (Olivera et al. 2012). While the 15xR012 population was not screened for resistance to JRCQC, all RILs were susceptible to TRTTF at the seedling stage (Fig. S3).

In addition to TRTTF, the population was susceptible to Ug99 races TTKSK and TTKTT. Of the *Pgt* isolates screened, only seedling resistance to TKTTF was segregating within the population. The results from our seedling stage screenings contradict previous reports of a pair of molecular markers, KASP_IWB72471 and KASP_IWB10558, being predictive of ASR genes *Sr11* and *Sr8155B1*, respectively (Nirmala et al. 2016; Nirmala et al. 2017). *Sr11*, residing on chromosome 6BL, confers resistance to *Pgt* race TKTTF (Green et al. 1960; Nirmala et al. 2016). However, the CItr 11390 was susceptible to TKTTF despite carrying the allele at KASP_IWB72471 reported to be predictive of *Sr11* resistance. Additionally, KASP_IWB72471 was found to have no effect on seedling resistance to TKTTF in single marker analysis, and *Sr11* was not detected by MQM for TKTTF or APR resistance despite substantial marker coverage in the region. Similarly, CItr 11390 was found to carry the allele reported to be predictive of *Sr8155B1* resistance at KASP_IWB10558 on chromosome 6AS.

However, CItr 11390, as well as MN07098-6 and the entire RIL population, were susceptible to race TTKTT, which is avirulent to Sr8155B1. These results indicate that KASP_IWB72471 and KASP_IWB10558 are not predictive of resistance at their respective loci in this population.

Initial analysis of the phenotypic data from seedling testing to race TKTTF indicated resistance was conferred by a single gene (Table 3). This was expected given the population segregates for *Sr7a*. However, MQM detected a second locus stretching approximately 50Mb on the long arm of chromosome 5A. Like *Sr7a*, the resistance allele at *QSr.umn-5A.1* was donated by the common wheat parent, MN07098-6. No known ASR genes are located on chromosome 5AL. Association mapping of North American wheat breeding germplasm by Bajgain et al. (2015a) detected three significant MTAs associated with seedling resistance to TKTTF on chromosome 5AL. Each of the three SNPs fall within the 95% Bayes credible interval of *QSr.umn-5A.1*, and one is located less than 3Mb from the peak of *QSr.umn-5A.1*. MN07098-6 was included among the association mapping panel used by Bajgain et al. (2015a), and the line carries the resistance allele at each of the three SNPs. The detection of co-locating QTL and MTAs sourced from common germplasm suggests the interval on chromosome 5AL may contain a novel source of resistance to *Pgt* race TKTTF.

Multiple QTL mapping detected a total of seven QTL for APR to *Pgt* in three of the four test environments. Among these QTL, two were detected in multiple environments that were both donated by CItr 11390. The largest effect QTL of the three, *QSr.umn-2A*, was detected in Kenya in 2019 and 2020. It is likely *QSr.umn-2A* is *Sr63*, an APR locus first reported by Mago et al. (2022) from the durum wheat (*Triticum turgidum* ssp. *durum*) variety 'Glossy Huguenot'. A KASP marker linked to *Sr63*, KASP_IWB32429, was located at the peak of *QSr.umn-2A* in both environments. Additionally, the physical positions of the *QSr.umn-2A* interval (681–702 Mb) were nearly identical to that of *Sr63* reported by Mago el al. (2022) in the RefSeq v2.1 assembly (683–696 Mb). The detected interval is distinct from the location of *Sr21* (713 Mb), and molecular marker screening confirmed the lack of the resistance allele at *Sr21* in CItr 11390. The detection of *QSr.umn-2A* and *Sr63* in a common environment (Kenya 2019) further supports the validation of *Sr63* as a unique APR locus on chromosome 2AL.

Given the population's apparent seedling susceptibility to Ug99 lineage races (Table 2), *Sr63* on chromosome 2AL could be an important target for resistance breeding to the Ug99 race group given its relatively large effect on disease reduction at the adult growth stages. The lack of detection of *Sr63* in Ethiopia indicates the gene may not be effective against other races present in Ethiopia, such as TRTTF and JRCQC. Screening the population in single-race nurseries could provide greater detail on efficacy of the gene to specific races. Additionally, APR genes have been found to provide pleiotropic resistance to the other cereal rusts, as well as other plant pathogens (Herrera-Foessel et al. 2014; Hiebert et al. 2010; Krattinger et al. 2009; Martinez et al. 2004; Rinaldo et al. 2017). Further disease resistance characterization of the 15xR012 RIL population to other pathogens, namely stripe rust (caused by *P. striiformis* f. sp. *tritici*) and leaf rust (caused by *P. triticina* f. sp. *tritici*) may be worth pursuing.

QSr.umn-6BL on the long arm of chromosome 6B was also detected in more than one environment. While the QTL was not retained in the multiple QTL model for Ken19, it was initially detected by both single-QTL and two-dimensional genome scans for Ken19, Ken20, and Eth20. The ASR gene *Sr11* resides on 6BL (Green et al. 1960), but molecular marker screening suggests that neither MN07098-6 nor CItr 11390 carry the resistance allele at *Sr11*. Additionally, the nearest flanking marker of *QSr.umn-6BL* was more than 40 Mb from *Sr11*. Bajgain et al. (2015a) previously reported a marker trait association (MTA) on chromosome 6BL at IWB35697 for APR in both Kenya and Ethiopia. MTAs in close proximity to IWB35697 were also detected in winter and durum wheat diversity panels in multiple years in Kenya and Ethiopia (Megeressa et al. 2020; Yu et al. 2012). However, local alignment of the significant markers from each of the aforementioned studies, including IWB35697, to RefSeq v2.1 revealed they were outside of the interval of *QSr.umn-6BL* and close to *Sr11*. The distance from *Sr11*, susceptibility of CItr 11390 to TKTTF, and the lack of APR QTL reported in this region suggest *QSr.umn-6BL* is a novel APR locus (Yu et al. 2014). Given the potential novelty of *QSr.umn-6BL*, refinement of the interval and the development of near isogenic lines (NILs) should be pursued to determine whether the QTL is a valuable breeding target for stem rust adult

plant resistance. Efforts to do so can be initiated using the genotyping assays developed in this study (Table S7). Additional assays that more closely approximate the intervals detected during MQM are needed.

In addition to the two QTL identified in multiple environments, five QTL were detected in single environments. Of these, four were contributed by the hexaploid parent MN07098-6: *QSr.umn-1A* (Eth20), *QSr.umn-3A* (Ken20), *QSr.umn-3B* (Ken20), and *QSr.umn-5A.2* (Ken19). *QSr.umn-1A* explained a large portion of the phenotypic variation observed in Ethiopia in 2020 (R^2 = 21.5). However, this is likely inflated by the small population size, relatively little phenotypic variation in the Eth20 environment, the lack of effectiveness of other loci such as *Sr63*, and the absence of ASR loci in the population besides *Sr7a* and *QSr.umn-5A.1*. While no known APR gene has been reported on 1AS, other QTL within the first ~ 16 Mb of chromosome 1AS have been detected in multiple studies (Bajgain et al. 2015b; Bansal et al. 2008; Bhavani et al. 2011; Yu et al. 2012). Notably, Bajgain et al. (2015b) detected a QTL in another University of Minnesota hard red spring wheat line for field resistance in 2013 in Kenya that co-locates with *QSr.umn-1A*.

QSr.umn-3A (R^2 = 5.0) was detected in Ken20 on the long arm of chromosome 3A with resistance conferred by the allele from MN07098-6. *Sr35* is the most well-known stem rust resistance loci on chromosome 3AL (Zhang et al. 2010). However, it is unlikely that *QSr.umn-3A* is *Sr35* as MN07098-6 is susceptible to TTKSK, the nearest flanking marker of *QSr.umn-3A* is ~ 11Mb from *Sr35*, and the pedigree of MN07098-6 lacks *T. monococcum* introgressions. *QSr.umn-3A* is also unlikely to be *Sr27*, which is carried on a 3AL.3RS translocation derived from the rye (*Secale cereale* L.) variety 'Imperial' (Marais 2001). *Sr27* provides strong seedling resistance to TTKSK that likely would have been detected during screening. Additionally, the deployment of the 3AL.3RS translocation has been almost exclusive to triticale (Singh et al. 2011). An MTA within 5 Mb of *QSr.umn-3A* was reported by Letta et al. (2013). However, this association was detected in a durum wheat panel grown in an Ethiopian nursery. In common wheat, the only APR QTL reported to partially overlap with *QSr.umn-3A* was detected in a CIMMYT biparental population grown in Njoro, Kenya during the 2011 main season (Singh et al. 2013). Further testing is needed to verify *QSr.umn-3A* given the limited reports of stem rust APR QTL within or near the interval.

QSr.umn-3B (R^2 = 6.6) was detected in Ken20 in the centromeric region of the long arm of chromosome 3B. The interval is in close proximity to a KASP marker linked to an NB-LRR motif within the *Sr12* locus that co-segregates with seedling stage resistance (Hiebert et al. 2016). The population is fixed for the allele linked to resistance at this *Sr12* (Table 1). However, adult plant resistance to Ug99 lineage and North American *Pgt* races also co-segregates with *Sr12* (Hiebert et al. 2016; Rouse et al. 2014). The co-localization of *QSr.umn-3B* with the aforementioned loci suggests it may be the same source of APR. Hiebert et al. (2016) also determined that the APR locus within *Sr12* interval interacted with *Sr57/Lr34/Yr18*. Due to the inability to include *Sr57/Lr34/Yr18* in QTL mapping, such interactions could not be evaluated while fitting multiple QTL models. Development and testing of additional genetic resource, such as families of NILs carrying various allelic combinations at the two loci, is necessary to further evaluate the effect of *QSr.umn-3B* and determine whether the locus interacts with *Sr57/Lr34/Yr18*.

QSr.umn-5A.2 (R^2 = 8.6) was detected in Ken19 on the long arm of chromosome 5A. During the 2013 off-season in Ethiopia, Bajgain et al. (2015a) detected a single MTA associated with APR that is ~ 13Mb from the peak marker of *QSr.umn-5A* lines. QTL on the chromosome 5AL associated with APR in African stem rust nurseries have also been reported in CIMMYT germplasm (Bhavani et al. 2011). Additionally, Edae et al. (2018) detected MTAs near the MTA reported by Bajgain et al. (2015a) for both infection response and disease severity to race QTHJC across three growing seasons in Minnesota using the same panel of spring wheat lines. As previously discussed, a QTL providing ASR to TKTTF was also detected in this study that co-localized with *QSr.umn-5A.1*. In the case of both QTL, the resistance allele was provided by MN07098-6. Given *QSr.umn.5A.1* was only detected in a single environment, further testing is needed to validate the QTL and also determine the mechanism for co-localization of ASR and APR much like the *Sr12* locus.

The last QTL detected in this study, *QSr.umn-6BS* (R^2 = 16.2), was detected only in Ken20 and contributed by CItr 11390. The effect of *QSr.umn-6BS* was relative small compared to the other QTL detected in Ken20. Additionally, an interaction

between this QTL and *Sr63* was detected during MQM. The mean CI value for lines carrying the resistance allele at both *QSr.umn-6BS* and *Sr63* was not significantly different from those only carrying the resistance allele at *Sr63*. This suggests that the presence of the resistance allele at *Sr63* masks the effect of *QSr.umn-6BS* and is sufficient to reduce disease symptoms. Given the observed masking effect, as well as the substantially larger effect and detection in multiple environments of *Sr63*, there is little reason to prioritize further investigations and selection of *QSr.umn-6BS*.

Stacking multiple APR genes is an effective approach to developing high levels of resistance to stem rust (Pretorius et al. 2017). The mean CI of RILs carrying three resistance alleles at *Sr57/Lr34/Yr18, Sr63*, and *QSr.umn-6BL* was markedly lower across environments compared to those carrying resistance alleles at zero, one, or two of the loci (Fig. 5, Table S6). However, developing pyramids of favorable stem rust resistance alleles from alien sources that are accessible for commercial breeding is challenging due to issues associated with interspecific hybridization such as linkage drag and chromosome pairing.

Sources for introgression are limited by the frequency of the resistance allele within a donor species. For example, of the 155 CIMMYT durum lines Mago et al. (2022) screened for *Sr63*, two were found to carry the resistance allele, making CItr 11390 only the third wheat accession known to carry the resistance allele at this locus. The RILs of the 15xR012 population are therefore the first hexaploid wheat lines known to carry *Sr63*. This is also likely the case for *QSr.umn-6BL*, as this is the first report of QTL for stem rust APR within this region. Multiple euploid RILs carry the resistance allele at *Sr7a* and *Sr57/Lr34/Yr18* in addition to *Sr63* and *QSr.umn-6BL* (Table S9).

The development and discovery of these lines demonstrates the feasibility of simultaneously mapping and transferring QTL from Khorasan wheat into hexaploid breeding materials. The RILs and SNP genotyping assays developed in this study provide value not only to targeted breeding efforts in areas where Ug99 stem rust races are present, but also facilitate the rapid deployment of newly validated and discovered loci such as *Sr63* and *QSr.umn-6BL* to the greater wheat breeding community.

Declarations

Funding

This project was supported by the USDA National Institute of Food and Agriculture competitive grant no. 2022-68013-36439, USDA-ARS appropriated project “Surveillance, Pathogen Biology, and Host Resistance of Cereal Rusts”, and the USDA-ARS National Plant Disease Recovery System.

Author Contributions

MF coordinated sequencing, constructed the genetic map, performed data analysis, and wrote the final manuscript. EC conducted molecular marker genotyping, aided in sequencing library preparation, and contributed to data analysis. ZK and AG coordinated field trials and oversaw data collection. MR conceived the study, developed the 15xR012 mapping population, facilitated seedling disease screenings, and aided in trial design. JA contributed to data analysis and provided suggestions to experimental design. All authors reviewed the manuscript.

Acknowledgments

This project was supported by the USDA National Institute of Food and Agriculture competitive grant no. 2022-68013-36439, USDA-ARS appropriated project “Surveillance, Pathogen Biology, and Host Resistance of Cereal Rusts”, and the USDA-ARS National Plant Disease Recovery System.

Data Availability

Phenotypic and genotypic data used for analysis are included in this article and supplementary files.

References

1. Bajgain P, Rouse M, Bulli P, et al (2015a) Association mapping of North American spring wheat breeding germplasm reveals loci conferring resistance to Ug99 and other African stem rust races. BMC Plant Biology 15
2. Bajgain P, Rouse MN, Bhavani S, Anderson JA (2015b) QTL mapping of adult plant resistance to Ug99 stem rust in the spring wheat population RB07/MN06113-8. Molecular Breeding 35
3. Bansal U, Bariana H, Wong D, et al (2014) Molecular mapping of an adult plant stem rust resistance gene Sr56 in winter wheat cultivar Arina. Theoretical and Applied Genetics 127:1441–1448
4. Bansal UK, Bossolini E, Miah H, et al (2008) Genetic mapping of seedling and adult plant stem rust resistance in two European winter wheat cultivars. Euphytica 164:821–828
5. Bates D, Mächler M, Bolker B, Walker S (2015) Fitting Linear Mixed-Effects Models Using lme4. Journal of Statistical Software 67:1–48
6. Bhavani S, Singh R, Argillier O, et al (2011) Mapping durable adult plant stem rust resistance to the race Ug99 group in six CIMMYT wheats. 2011 Borlaug Global Rust Initiative Technical Workshop 43–53
7. Bradbury PJ, Zhang Z, Kroon DE, et al (2007) TASSEL: software for association mapping of complex traits in diverse samples. Bioinformatics 23:2633–2635
8. Braun HJ, Atlin G, Payne T (2010) Multi-location testing as a tool to identify plant response to global climate change
9. Briggs J, Chen S, Zhang W, et al (2015) Mapping of *SrTm4*, a Recessive Stem Rust Resistance Gene from Diploid Wheat Effective to Ug99. Phytopathology® 105:1347–1354
10. Broman KW, Wu H, Sen Ś, Churchill GA (2003) R/qtl: QTL mapping in experimental crosses. Bioinformatics 19:889–890
11. Chen S, Zhang W, Bolus S, et al (2018) Identification and characterization of wheat stem rust resistance gene Sr21 effective against the Ug99 race group at high temperature. PLOS Genetics 14:e1007287
12. Edae EA, Pumphrey MO, Rouse MN (2018) A Genome-Wide Association Study of Field and Seedling Response to Individual Stem Rust Pathogen Races Reveals Combinations of Race-Specific Genes in North American Spring Wheat. Frontiers in Plant Science 9
13. Elshire RJ, Glaubitz JC, Sun Q, et al (2011) A Robust, Simple Genotyping-by-Sequencing (GBS) Approach for High Diversity Species. PLoS ONE 6:e19379
14. FAO (2022) Crop Prospects and Food Situation. Food and Agriculture Organization of the United Nations
15. Gao L, Babiker EM, Nava IC, et al (2019) Temperature-sensitive wheat stem rust resistance gene Sr15 is effective against Puccinia graminis f. sp. tritici race TTKSK. Plant Pathology 68:143–151
16. Gao L, Turner MK, Chao S, et al (2016) Genome Wide Association Study of Seedling and Adult Plant Leaf Rust Resistance in Elite Spring Wheat Breeding Lines. PLOS ONE 11:e0148671
17. Gill BS, Friebe B, Endo TR (1991) Standard karyotype and nomenclature system for description of chromosome bands and structural aberrations in wheat (Triticum aestivum). Genome 34:830–839
18. Gill BS, Raupp WJ (1987) Direct Genetic Transfers from Aegilops squarrosa L. to Hexaploid Wheat. Crop Science 27:445–450
19. Godfray HCJ, Beddington JR, Crute IR, et al (2010) Food Security: The Challenge of Feeding 9 Billion People. Science 327:812–818

20. Grassini P, Eskridge KM, Cassman KG (2013) Distinguishing between yield advances and yield plateaus in historical crop production trends. Nature Communications 4
21. Green GJ, Knott DR, Watson IA, Pugsley AT (1960) Seedling reactions to stem rust of lines of Marquis wheat with substituted genes for rust resistance. Canadian Journal of Plant Science 40:524–538
22. Hayes HK, Ausemus ER, Stakman EC, et al (1936) Thatcher Wheat
23. Helguera M, Khan IA, Kolmer J, et al (2003) PCR Assays for the *Lr37-Yr17-Sr38* Cluster of Rust Resistance Genes and Their Use to Develop Isogenic Hard Red Spring Wheat Lines. Crop Science 43:1839–1847
24. Herrera-Foessel SA, Singh RP, Lillemo M, et al (2014) Lr67/Yr46 confers adult plant resistance to stem rust and powdery mildew in wheat. Theoretical and Applied Genetics 127:781–789
25. Hiebert CW, Kolmer JA, Mccartney CA, et al (2016) Major Gene for Field Stem Rust Resistance Co-Locates with Resistance Gene Sr12 in 'Thatcher' Wheat. PLOS ONE 11:e0157029
26. Hiebert CW, Thomas JB, Mccallum BD, et al (2010) An introgression on wheat chromosome 4DL in RL6077 (Thatcher*6/PI 250413) confers adult plant resistance to stripe rust and leaf rust (Lr67). Theoretical and Applied Genetics 121:1083–1091
27. Kalous JR, Martin JM, Sherman JD, et al (2015) Impact of the D genome and quantitative trait loci on quantitative traits in a spring durum by spring bread wheat cross. Theoretical and Applied Genetics 128:1799–1811
28. Kimber G, Sears ER (1968) Nomenclature for the description of aneuploids in the Triticinae. 3rd International Wheat Genetics Symposium 468–473
29. Kislev ME (1982) Stem Rust of Wheat 3300 Years Old Found in Israel. Science 216:993–994
30. Knott DR (1962) The inheritance of rust resistance: IX. The inheritance of resistance to races 15B and 56 of stem rust in the wheat variety Khapstein. Canadian Journal of Plant Science 42:415–419
31. Knott DR (2000) The inheritance of stem rust resistance in Thatcher wheat. Canadian Journal of Plant Science 80:53–63
32. Kolmer JA (1996) Genetics of resistance to wheat leaf rust. Annual Review of Phytopathology 34:435–455
33. Kosambi DD (1943) The estimation of map distances from recombination values. Annals of Eugenics 12:172–175
34. Kosgey ZC, Edae EA, Dill-Macky R, et al (2021) Mapping and Validation of Stem Rust Resistance Loci in Spring Wheat Line CI 14275. Frontiers in Plant Science 11
35. Krattinger SG, Lagudah ES, Spielmeyer W, et al (2009) A Putative ABC Transporter Confers Durable Resistance to Multiple Fungal Pathogens in Wheat. Science 323:1360–1363
36. Kumar S, Fetch TG, Knox RE, et al (2021) Mapping of Ug99 stem rust resistance in Canadian durum wheat. Canadian Journal of Plant Pathology 43:599–611
37. Lanning SP, Blake NK, Sherman JD, Talbert LE (2008) Variable Production of Tetraploid and Hexaploid Progeny Lines from Spring Wheat by Durum Wheat Crosses. Crop Science 48:199–202
38. Laugerotte J, Baumann U, Sourdille P (2022) Genetic control of compatibility in crosses between wheat and its wild or cultivated relatives. Plant Biotechnology Journal 20:812–832
39. Leigh FJ, Wright TIC, Horsnell RA, et al (2022) Progenitor species hold untapped diversity for potential climate-responsive traits for use in wheat breeding and crop improvement. Heredity 128:291–303
40. Letta T, Maccaferri M, Badebo A, et al (2013) Searching for novel sources of field resistance to Ug99 and Ethiopian stem rust races in durum wheat via association mapping. Theoretical and Applied Genetics 126:1237–1256
41. Li H (2011) A statistical framework for SNP calling, mutation discovery, association mapping and population genetical parameter estimation from sequencing data. Bioinformatics 27:2987–2993
42. Li H, Handsaker B, Wysoker A, et al (2009) The Sequence Alignment/Map format and SAMtools. Bioinformatics 25:2078–2079

43. Mago R, Chen C, Xia X, et al (2022) Adult plant stem rust resistance in durum wheat Glossy Huguenot: mapping, marker development and validation. Theoretical and Applied Genetics 135:1541–1550
44. Manichaikul A, Moon JY, Sen S, et al (2009) A Model Selection Approach for the Identification of Quantitative Trait Loci in Experimental Crosses, Allowing Epistasi. Genetics 181:1077–1086
45. Marais GF (2001) An evaluation of three Sr27-carrying wheat × rye translocations. South African Journal of Plant and Soil 18:135–136
46. Martin M (2011) Cutadapt removes adapter sequences from high-throughput sequencing reads. EMBnet.journal 17:10
47. Martínez F, Niks RE, Singh RP, Rubiales D (2001) Characterization of Lr46, a Gene Conferring Partial Resistance to Wheat Leaf Rust. Hereditas 135:111–114
48. McFadden ES (1930) A successful transfer of emmer characters to vulgare wheat. Journal of the American Society of Agronomy 22:1020–1034
49. McIntosh RA, Dubcovsky J, Rogers WJ, et al (2020) Catalogue of Gene Symbols for Wheat: 2020 Supplement. Annual Wheat Newsletter 66
50. McIntosh RA, Wellings CR, Park RF (1995) Wheat Rusts: An Atlas of Resistance Genes
51. Megerssa SH, Ammar K, Acevedo M, et al (2020) Multiple-Race Stem Rust Resistance Loci Identified in Durum Wheat Using Genome-Wide Association Mapping. Frontiers in Plant Science 11
52. Money D, Gardner K, Migicovsky Z, et al (2015) LinkImpute: Fast and Accurate Genotype Imputation for Nonmodel Organisms. G3 Genes|Genomes|Genetics 5:2383–2390
53. Mustahsan W (2022) Characterization of stripe rust resistance and yield-related traits in an 'Overley' x 'Overland' population. Thesis
54. Nirmala J, Chao S, Olivera P, et al (2016) Markers Linked to Wheat Stem Rust Resistance Gene Sr11 Effective to Puccinia graminis f. sp. tritici Race TKTTF. Phytopathology 106:1352–1358
55. Nirmala J, Saini J, Newcomb M, et al (2017) Discovery of a Novel Stem Rust Resistance Allele in Durum Wheat that Exhibits Differential Reactions to Ug99 Isolates. G3 Genes|Genomes|Genetics 7:3481–3490
56. Olivera P, Newcomb M, Szabo LJ, et al (2015) Phenotypic and Genotypic Characterization of Race TKTTF of Puccinia graminis f. sp. tritici that Caused a Wheat Stem Rust Epidemic in Southern Ethiopia in 2013–14. Phytopathology® 105:917–928
57. Olivera PD, Jin Y, Rouse M, et al (2012) Races of Puccinia graminis f. sp. tritici with Combined Virulence to Sr13 and Sr9e in a Field Stem Rust Screening Nursery in Ethiopia. Plant Disease 96:623–628
58. Olivera PD, Villegas D, Cantero-Martínez C, et al (2022) A unique race of the wheat stem rust pathogen with virulence on *Sr31* identified in Spain and reaction of wheat and durum cultivars to this race. Plant Pathology 71:873–889
59. Olson EL, Rouse MN, Pumphrey MO, et al (2013a) Introgression of stem rust resistance genes SrTA10187 and SrTA10171 from Aegilops tauschii to wheat. Theoretical and Applied Genetics 126:2477–2484
60. Olson EL, Rouse MN, Pumphrey MO, et al (2013b) Simultaneous transfer, introgression, and genomic localization of genes for resistance to stem rust race TTKSK (Ug99) from Aegilops tauschii to wheat. Theoretical and Applied Genetics 126:1179–1188
61. Oróstica KY, Verdugo RA (2016) chromPlot: visualization of genomic data in chromosomal context. Bioinformatics 32:2366–2368
62. Patpour M, Justesen AF, Tecle AW, et al (2020) First Report of Race TTRTF of Wheat Stem Rust (Puccinia graminis f. sp. tritici) in Eritrea. Plant Disease 104:973
63. Peterson RF, Campbell AB, Hannah AE (1948) A diagrammatic scale for estimating rust intensity on leaves and stems of cereals. Canadian Journal of Research 26c:496–500

64. Poland JA, Brown PJ, Sorrells ME, Jannink J-L (2012) Development of High-Density Genetic Maps for Barley and Wheat Using a Novel Two-Enzyme Genotyping-by-Sequencing Approach. PLoS ONE 7:e32253
65. Pretorius ZA, Ayliffe M, Bowden RL, et al (2017) Advances in control of wheat rusts. Achieving sustainable cultivation of wheat 1:295–343
66. Pretorius ZA, Jin Y, Bender CM, et al (2012) Seedling resistance to stem rust race Ug99 and marker analysis for Sr2, Sr24 and Sr31 in South African wheat cultivars and lines. Euphytica 186:15–23
67. Pretorius ZA, Singh RP, Wagoire WW, Payne TS (2000) Detection of Virulence to Wheat Stem Rust Resistance Gene Sr31 in Puccinia graminis f. sp. tritici in Uganda. Plant Disease 84:203–203
68. Quinlan AR, Hall IM (2010) BEDTools: a flexible suite of utilities for comparing genomic features. Bioinformatics 26:841–842
69. Rinaldo A, Gilbert B, Boni R, et al (2017) The Lr34 adult plant rust resistance gene provides seedling resistance in durum wheat without senescence. Plant Biotechnology Journal 15:894–905
70. Roelfs AP (1985) Wheat and rye stem rust. The Cereal Rusts, Vol. 2 2:3–37
71. Roelfs AP, Martens JWM (1988) An international system of nomenclature for Puccinia graminis f.sp. tritici. Phytopathology 78:526–533
72. Roelfs AP, Singh RP, Saari EE (1992) Rust Diseases of Wheat: Concepts and Methods of Disease Management.
73. Rouse MN, Talbert LE, Singh D, Sherman JD (2014) Complementary epistasis involving Sr12 explains adult plant resistance to stem rust in Thatcher wheat (Triticum aestivum L.). Theoretical and Applied Genetics 127:1549–1559
74. Rouse MN, Wanyera R, Njau P, Jin Y (2011) Sources of Resistance to Stem Rust Race Ug99 in Spring Wheat Germplasm. Plant Disease 95:762–766
75. Rowland GG, Kerber ER (1974) Telocentric mapping in hexaploid wheat of genes for leaf rust resistance and other characters derived from Aegilops squarrosa. Canadian Journal of Genetics and Cytology 16:137–144
76. Sharma HC, Gill BS (1983) Current status of wide hybridization in wheat. Euphytica 32:17–31
77. Singh N, Raupp J, Koo D-H, et al (2020) In-silico detection of aneuploidy and chromosomal deletions in wheat using genotyping-by-sequencing. Plant Methods 16
78. Singh RP, Hodson DP, Huerta-Espino J, et al (2011) The Emergence of Ug99 Races of the Stem Rust Fungus is a Threat to World Wheat Production. Annual Review of Phytopathology 49:465–481
79. Singh RP, Hodson DP, Jin Y, et al (2015) Emergence and Spread of New Races of Wheat Stem Rust Fungus: Continued Threat to Food Security and Prospects of Genetic Control. Phytopathology® 105:872–884
80. Singh RP, Huerta-Espino J (2003) Effect of leaf rust resistance gene Lr34 on components of slow rusting at seven growth stages in wheat. Euphytica 129:371–376
81. Singh S, Singh RP, Bhavani S, et al (2013) QTL mapping of slow-rusting, adult plant resistance to race Ug99 of stem rust fungus in PBW343/Muu RIL population. Theoretical and Applied Genetics 126:1367–1375
82. Stakman EC, Stewart DM, Loegering WQ (1962) Identification of physiologic races of Puccinia graminis var. tritici. E617
83. Stubbs RW, Prescott JM, Saari EE, Dubin HJ (1986) Cereal disease methodology manual
84. Stuthman DD, Leonard KJ, Miller-Garvin J (2007) Breeding Crops for Durable Resistance to Disease. 95:319–367
85. Suenaga K, Singh RP, Huerta-Espino J, William HM (2003) Microsatellite Markers for Genes Lr34/Yr18 and Other Quantitative Trait Loci for Leaf Rust and Stripe Rust Resistance in Bread Wheat. Phytopathology 93:881–890
86. Taylor J, Butler D (2017) R Package ASMap: Efficient Genetic Linkage Map Construction and Diagnosis. Journal of Statistical Software 79:1–29
87. Terefe TG, Visser B, and Pretorius ZA (2016) Variation in Puccinia graminis f. sp. tritici detected on wheat and triticale in South Africa from 2009 to 2013. Crop Protection 86:9–16

88. The TT (1973) Chromosome Location of Genes Conditioning Stem Rust Resistance Transferred from Diploid to Hexaploid Wheat. Nature New Biology 241:256–256
89. Turner MK, Jin Y, Rouse MN, Anderson JA (2016) Stem Rust Resistance in 'Jagger' Winter Wheat. Crop Science 56:1719–1725
90. Wu Y, Bhat PR, Close TJ, Lonardi S (2008) Efficient and Accurate Construction of Genetic Linkage Maps from the Minimum Spanning Tree of a Graph. PLoS Genetics 4:e1000212
91. Xu LS, Wang MN, Cheng P, et al (2013) Molecular mapping of Yr53, a new gene for stripe rust resistance in durum wheat accession PI 480148 and its transfer to common wheat. Theoretical and Applied Genetics 126:523–533
92. Yu L-X, Barbier H, Rouse MN, et al (2014) A consensus map for Ug99 stem rust resistance loci in wheat. Theoretical and Applied Genetics 127:1561–1581
93. Yu L-X, Morgounov A, Wanyera R, et al (2012) Identification of Ug99 stem rust resistance loci in winter wheat germplasm using genome-wide association analysis. Theoretical and Applied Genetics 125:749–758
94. Zhang W, Chen S, Abate Z, et al (2017) Identification and characterization of Sr13, a tetraploid wheat gene that confers resistance to the Ug99 stem rust race group. Proceedings of the National Academy of Sciences 114:E9483–E9492
95. Zhang W, Olson E, Saintenac C, et al (2010) Genetic Maps of Stem Rust Resistance Gene Sr35 in Diploid and Hexaploid Wheat. Crop Science 50:2464–2474
96. Zhu T, Wang L, Rimbert H, et al (2021) Optical maps refine the bread wheat Triticum aestivum cv. Chinese Spring genome assembly. The Plant Journal 107:303–314

Figures

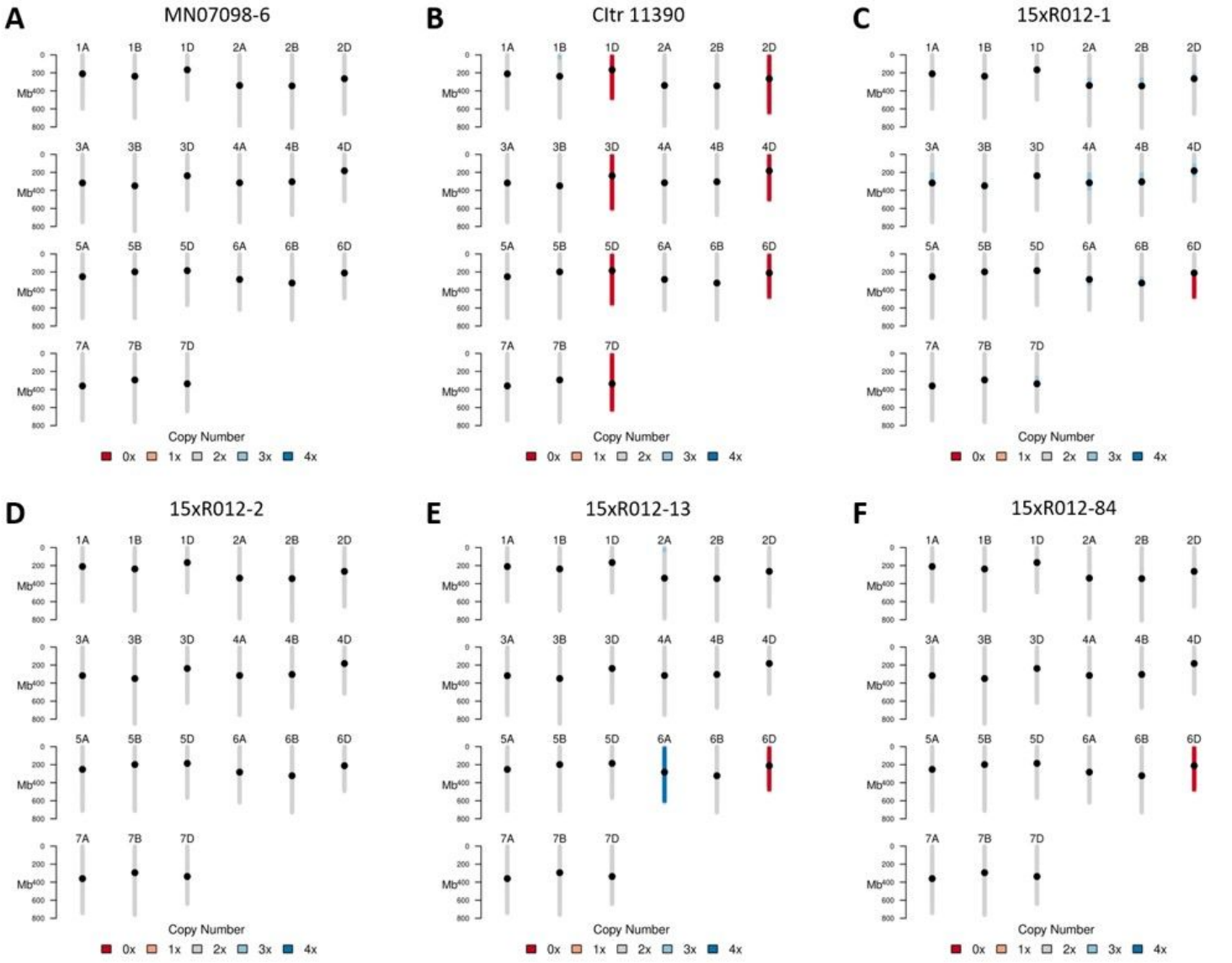


Figure 1

Karyotypes of MN07098-6, CItr 11390, and four representative RILs from the 15xR012 population with various ploidy states: **A)**hexaploid parent MN07098-6, **B)**tetraploid parent CItr 11390, **C)**ditelosomic 6AS 15xR012-1, **D)** hexaploid 15xR012-2, **E)** nullisomic-tetrasomic 6D/6A 15xR012-13, and **F)** nullisomic 6D 15xR012-84. Centromeres are represented by the black circles. Chromosome copy number is indicated by color.

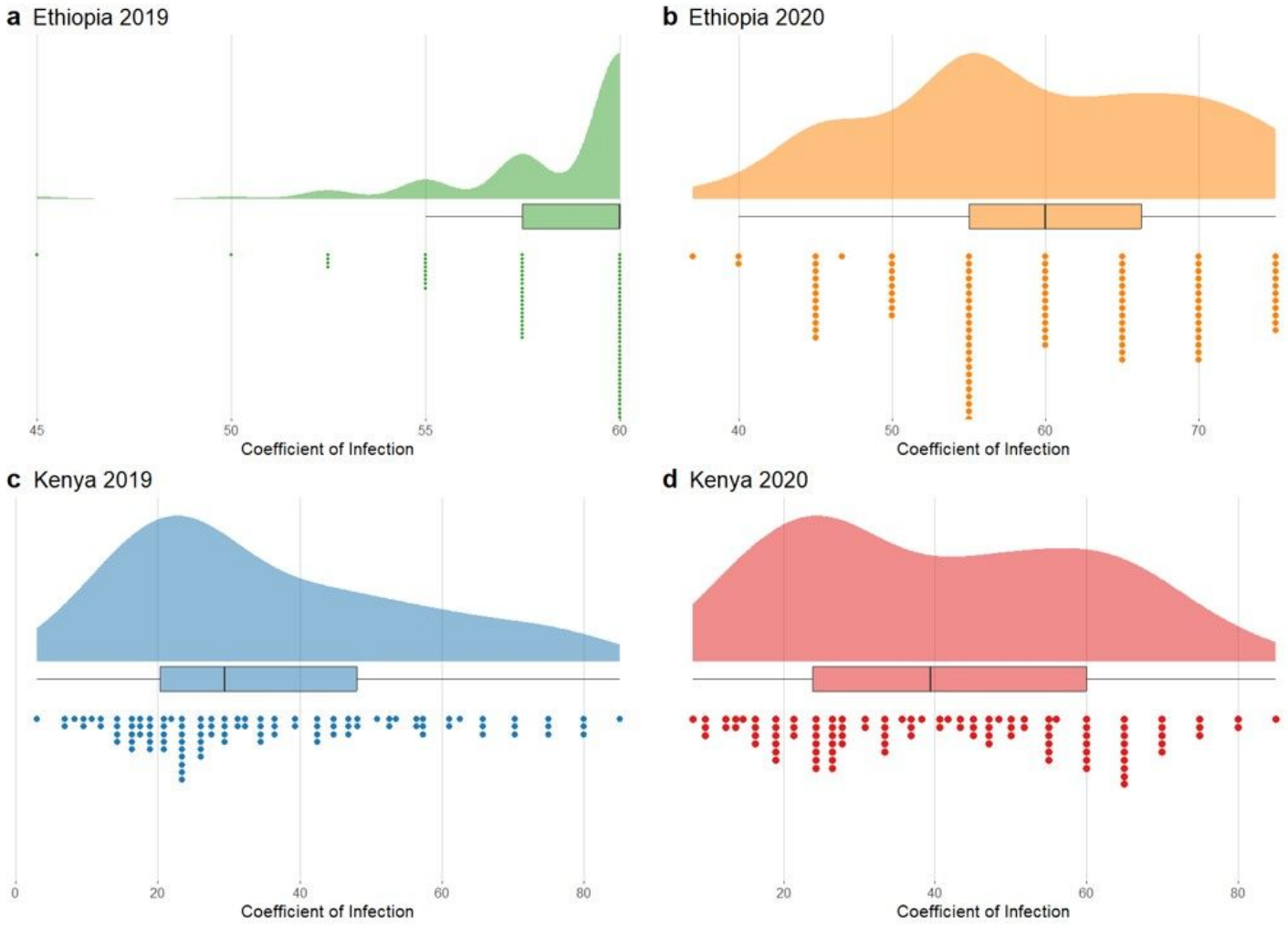


Figure 2

Distribution of stem rust coefficient of infection values (CI) for the 15xR012 population within **a)** Ethiopia 2019 (Eth19), **b)** Ethiopia 2020 (Eth20) ,**c)** Kenya 2019 (Ken19), and **d)** Kenya 2020 (Ken20). Data presented are mean CI values for each RIL before and after adjustment for the effect of *Sr57/Lr34/Yr18*.

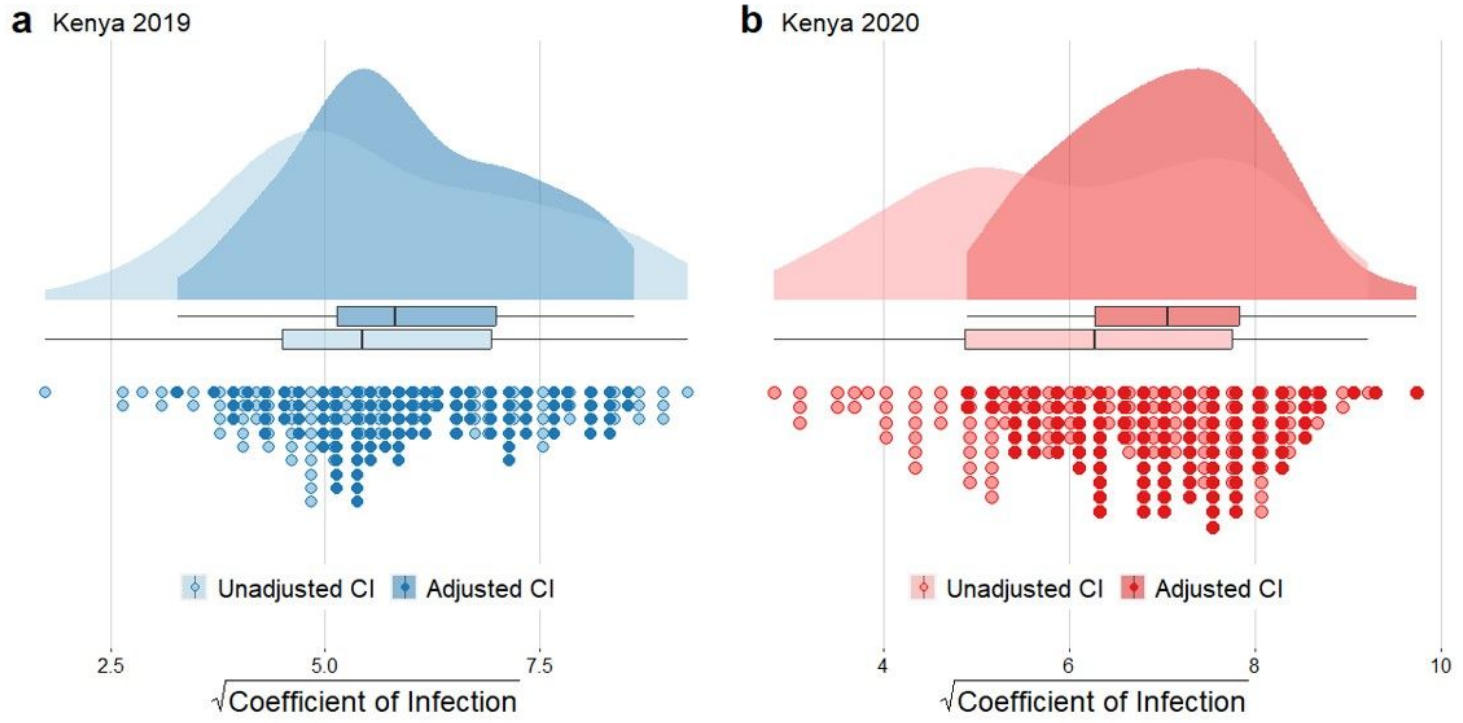


Figure 3

Distribution of stem rust coefficient of infection values (CI) for the 15xR012 population within **a)** Kenya 2019 (Ken19) and **b)** Kenya 2020 (Ken20). Data presented are mean CI values for each RIL after square root transformation and adjustment for the effect of *Sr57/Lr34/Yr18*

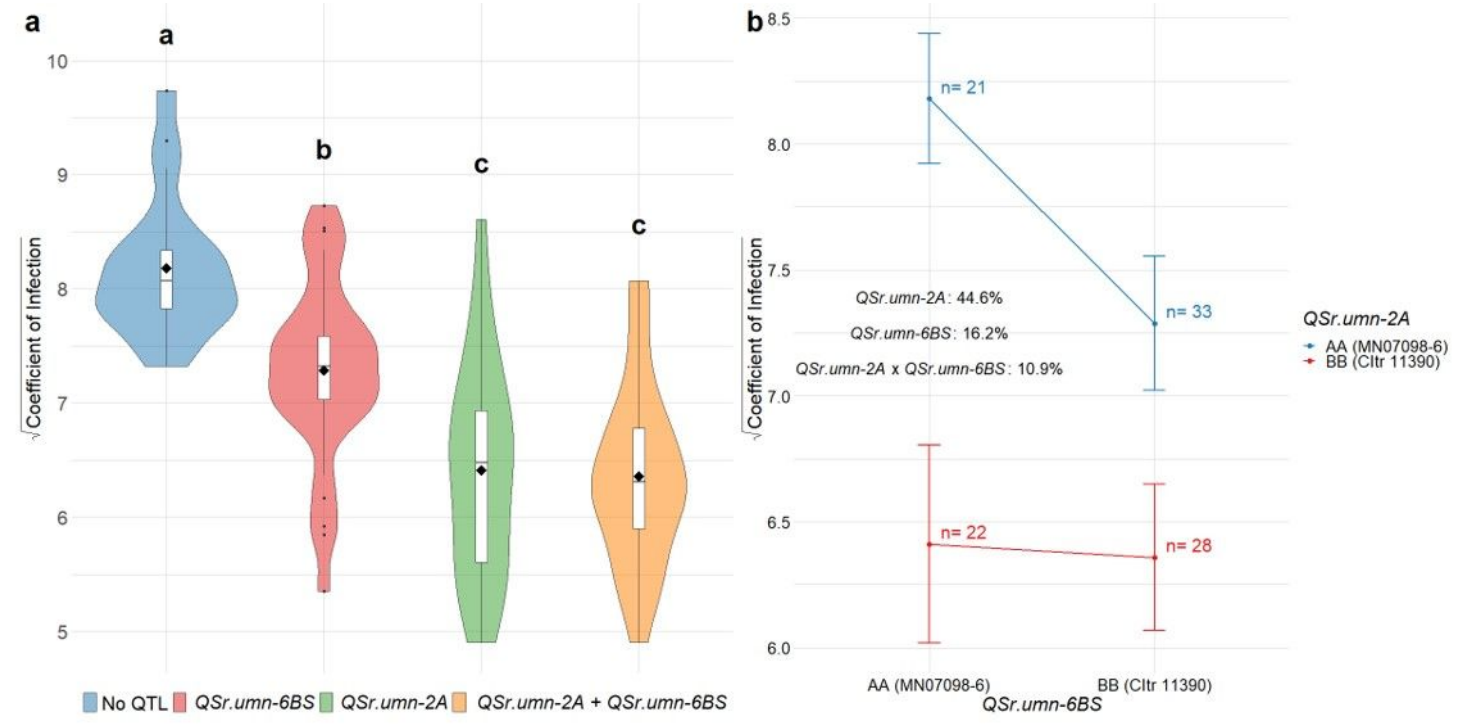


Figure 4

Epistatic interaction of QTL for stem rust coefficient of infection (CI) in the 15xR012 population. **a)** Distribution of the square root transformed CI values in Ken20 for each allelic combination of *QSr.umn-2A* and *QSr.umn-6BS* among the RIL population. **b)** Effect plot between *QSr.umn-2A* and *QSr.umn-6BS* in Ken20. The A allele is contributed by hexaploid parent MN07098-6, and the B allele is contributed by tetraploid parent CItr 11390. Black diamonds in panels A and C indicate mean values. Groups that do not share letters above the plot are significantly different ($p < 0.05$; Tukey's HSD). Percentages after the QTL names and the interaction term are the percent of variation explained. Error bars indicate the 95% confidence interval

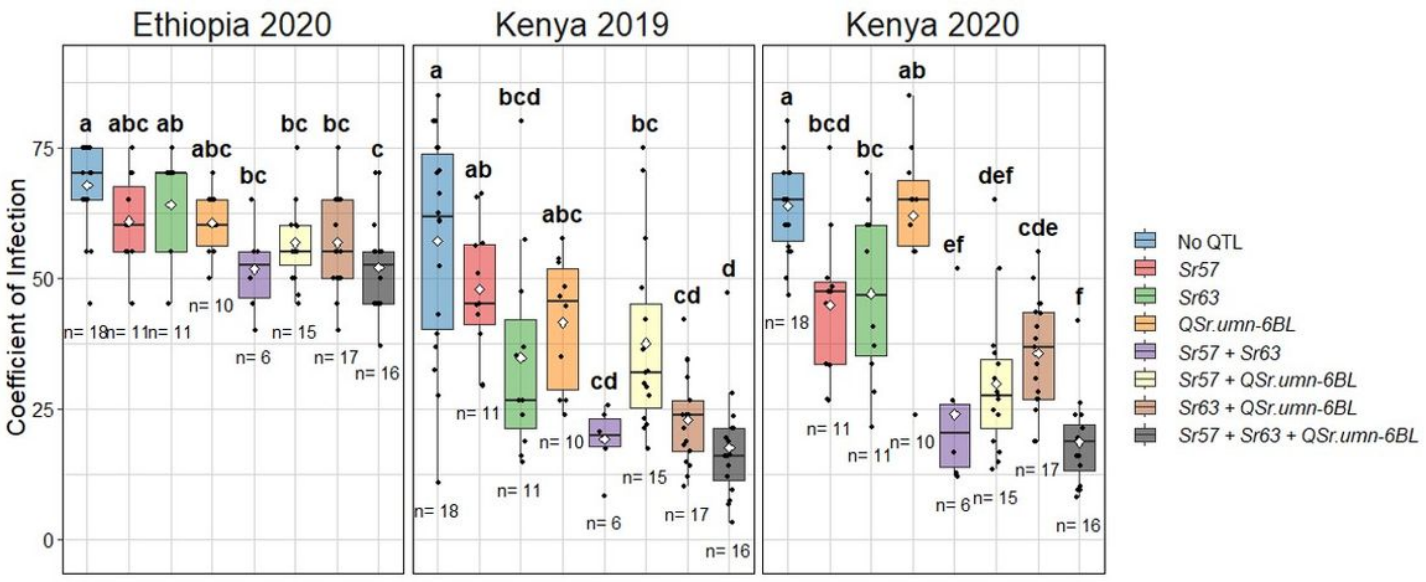


Figure 5

Unadjusted stem rust coefficient of infection among the 15xR012 RILs carrying each combination of *Sr57/Lr34/Yr18*, *Sr63*, and *QSr.umn-6BL* alleles within the three environments *QSr.umn-6BL* was detected. White diamonds indicate mean CI of each QTL combination within an environment. Groups within an environment that do not share letters above the plot are significantly different ($p < 0.05$; Tukey's HSD).

Supplementary Files

This is a list of supplementary files associated with this preprint. Click to download.

- FigureS2.pdf
- UMN15xR012AfricanRustGeneticMap.xlsx
- UMN15xR012AfricanRustPhenotypes.xlsx
- UMN15xR012AfricanRustSupplementalsFINAL.docx